

Structural, AC conductivity and dielectric properties of bulk 1,3-Dihydro-1,3,3-trimethylspiro[2H-indole-2,3'-[3H]naphth[2,1-b][1,4]oxazine]

W.M. Desoky

Physics Department, Faculty of Science, Zagazig University, Zagazig, Egypt

Received 25th Nov. 2018
Accepted 17th Apr. 2019

The frequency dependent of the AC conductivity and Dielectric properties of organic compound 1,3-Dihydro-1,3,3-trimethylspiro [2H-indole-2,3'-[3H] naphth [2,1-b] [1,4] oxazine], SPO, have been studied as a bulk in a frequency range (50 Hz–5 MHz) with different temperature. X-ray diffraction (XRD) and high-resolution transmission electron microscope (HRTEM) suggest that the SPO compound has polycrystalline with monoclinic structure, space group P21 along with crystalline size around 35 nm at room temperature. The obtained results of AC conductivity, $\sigma(\omega)$, increased with increasing frequency. Consequently, the exponent frequency factor, S , was estimated and found to be $S < 1$ and increase with increasing temperature. This behavior indicates that the small Polaron (SP) model is the most predominated conduction mechanism. The dielectric properties including dielectric constant, dielectric loss and loss tangent were found to be decreased with increasing frequency, while these parameters are increased with increasing the temperature in the investigated ranges. Moreover, the activation energy, the relaxation time and the maximum barrier height were extracted.

Keywords: Spirooxazine, Photochromic material, Dielectric properties and organic material

Introduction

In recent years, organic photochromic colourant materials, such as Spirooxazine (SPO), have been amply investigated due to their molecular structure and the potential application in optical systems and the optoelectronics device fabrication [1-7]. Spirooxazine (SPO) is recognized as photochromic compounds, which distinguished by their preferable properties of chemical stability, photoresponse, fatigue resistance and resolving power [8]. The reversible photochromic process of spirooxazine by cause of the heterolytic cleavage and reverting of C-O bond, in which colored form is generated and detect a red shift after UV irradiation in the absorption spectrum [9]. The SPO compounds usually showed photochromism behavior in various forms such as solution, polymer medium while it usually found non-photochemically active in solid state

form at normal conditions [9]. This response limitation of solid-state of the compound due to the large structural changes accompanying the ring opening mechanism. Generally, the changeable of optical and dielectric properties of SPO compound give a good chance to fabricate new optoelectronic devices. In particular, the SPO compound has a massive number of potential applications such as UV sensors, optical delay generators, dosimeter, molecular switches, biosensors, optobioelectronics and systems for accumulation of solar energy [10-19]. On the other hand, Organic semiconductor compounds have several clear advantages in comparison with inorganic materials such as low cost of fabrication, easy preparation, mechanical elasticity and low-temperature process-ability [20-22]. AC impedance spectroscopy is a crucial tool for investigating the electrical properties of various materials and to interpret the nature of the

conduction mechanism of the solid forms. In addition, the behavior of dielectric polarization and dielectric relaxation of charge carriers in low mobility compounds such as organic compound provides information about the orientation and translational adjustment of mobile charge display in the dielectric medium [23]. The scope of this work is to investigate the crystalline structural properties of SPO compound using X-ray diffraction (XRD) and transmission electron microscopy (TEM) as powder form. Also, the AC conductivity behavior and the related dielectric properties of SPO pellet sandwiched between two gold electrodes (ohmic contact) with temperature and frequency dependence are investigated to determine the predominant conduction mechanism involved and obtain information about the activation energy and dielectric relaxation of charge carriers.

Al Technique

1,3-Dihydro-1,3,3-trimethylspiro [2H-indole-2,3'-[3H] naphth [2,1-b] [1,4] oxazine](SPO) was obtained from the Sigma Aldrich company and were used as it is without further purifications. The chemical structure of SPO compound is shown in figure (1). The fine powder of SPO compound was obtained using a mortar. Then, the powder was compressed in the pellet form under a pressure of $5 \times 10^5 \text{ N/m}^2$ by a suitable apparatus. The SPO pellet was sandwiched between two evaporated gold electrodes using thermal evaporation, Edward E306A, under vacuum of 10^{-4} Pa . The crystal structural characteristic of the powder was studied using an X-ray diffractometer (Philip model X'pert) with utilized monochromatic $\text{CuK}\alpha$ radiation ($\lambda = 1.54 \text{ \AA}$) with a scanning rate 2° min^{-1} . Also, the high-resolution transmission electron microscope (HRTEM) model "JEOLJEM-2100" was used to investigate the grain shape and size of powder form, the powder was loaded on TEM copper grid with carbon coated using suspension method in ethylene glycol. The AC measurements were scrutinized using an automatic RLC bridge, Hioki 3532 in the frequency range from 50 Hz to 5 MHz. The sample was holed in a holder specially designed to minimize stray capacitance. For the electrical contact, the copper wires were connected to the pellet electrodes using a conductive silver past. The temperature of the sample was recognized by type-K thermocouple. The impedance, Z, the capacitance, C, and the phase

angle, θ , were measured for SPO sample with different frequency and temperature. The AC conductivity was calculated using the following formula: $\sigma(\omega) = d/ZA$, where A is the cross-sectional area and F is the thickness of the sample. The dielectric constant, ϵ' , was calculated from the formula: $\epsilon' = dC/A\epsilon_0$, where ϵ_0 is the free space permittivity. The loss tangent, $\tan \delta$, where $\delta = 90 - \theta$, and the dielectric loss, $\epsilon'' = \epsilon_1 \tan \delta$ [23].

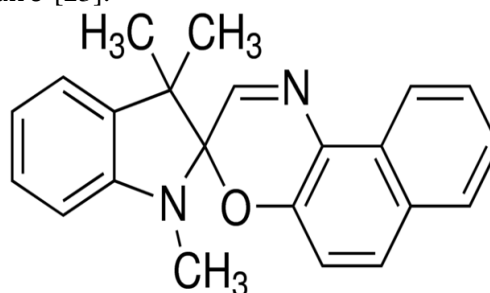


Figure (1): The molecular structure of 1,3-Dihydro-1,3,3-trimethylspiro[2H-indole-2,3'-[3H]naphth[2,1-b][1,4]oxazine] (SPO)

Results And Discussion

The SPO compound structure was studied as a powder form using XRD as shown in Fig. (2). This figure shows a polycrystalline structure. The indexing of Miller indices of all peaks and the lattice constants of SPO were calculated using the CRYSFIRE&CHECKCELL computer programs [24,25]. The results suggest that the SPO compound has a monoclinic structure with space group P21. The lattice constants a, b, c was extracted as 13.120 \AA , 8.038 \AA , 6.070 \AA , and angles α , β and γ are 90, 96.37, and 90 respectively.

The crystallite size, D, and the strain, ϵ , were evaluated using the Size-strain plot method equation as follow [26]: -

$$(d_{hkl} \beta_{hkl} \cos \theta)^2 = \frac{K}{D} (d_{hkl}^2 \beta_{hkl} \cos \theta) + \left(\frac{\epsilon}{2}\right)^2 \quad (1)$$

where d, β and K are the interplanar distance, full width half maximum and constant respectively. In addition, the dislocation density was calculated from the relation:

$$\delta = \frac{1}{D^2} \quad (2)$$

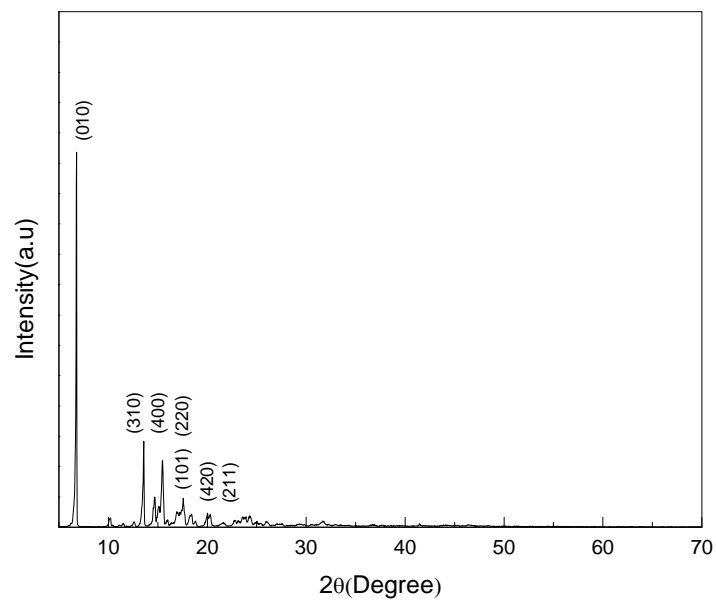


Figure (2): XRD pattern of SPO compound in a powder form

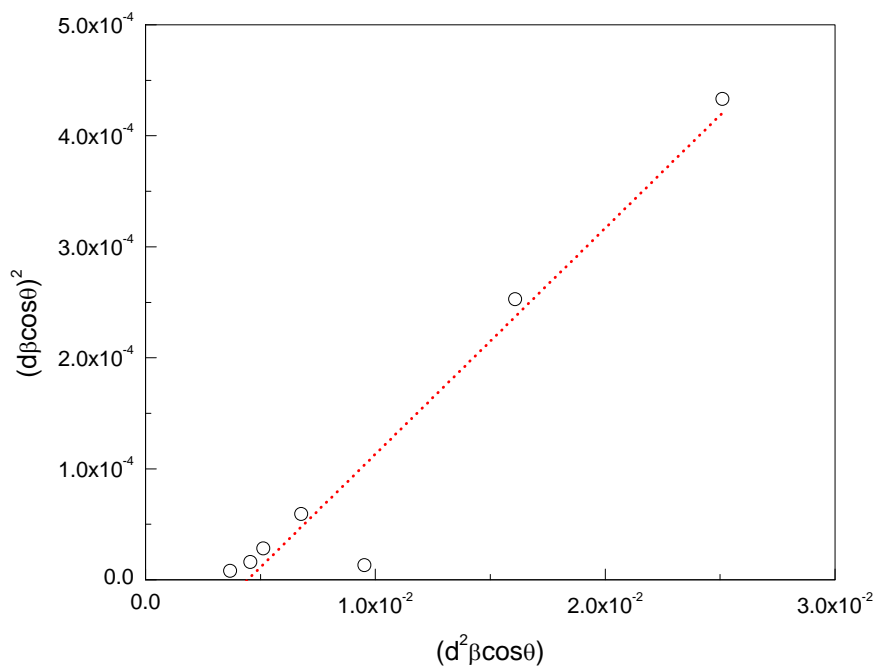


Figure (3): The Size-strain plot of SPO compound as a powder form at room temperature

Concerning to equation (1) and Figure (3), the crystallite size and the strain are extracted from the slope and the root of the intercept of y-axis of the linear fitted data, respectively. The values of D , ϵ and δ are found to be 34 nm, 67.2×10^{-4} and 1.04×10^{15} line/m², respectively. The high-resolution transmission electron microscope (HRTEM) has been used to investigate the powder form of SPO compound with different magnification as illustrated in Figure (4). This figure affirms the formation of nano-crystalline with diameter range between 30 to 40 nm. This value is in good agreement with that obtained from XRD results.

AC conductivity measurement is an essential tool to inspect the dielectric properties such as dielectric constant, dielectric loss and loss tangent. In addition, the AC conductivity data may scrutinize the conduction mechanism involved in the investigated system.

The AC conductivity and the dielectric properties were characterized at different frequencies in the range between 50 Hz to 5 MHz. Figure (5) represents the frequency dependence of the AC conductivity at different temperature for SPO compound.

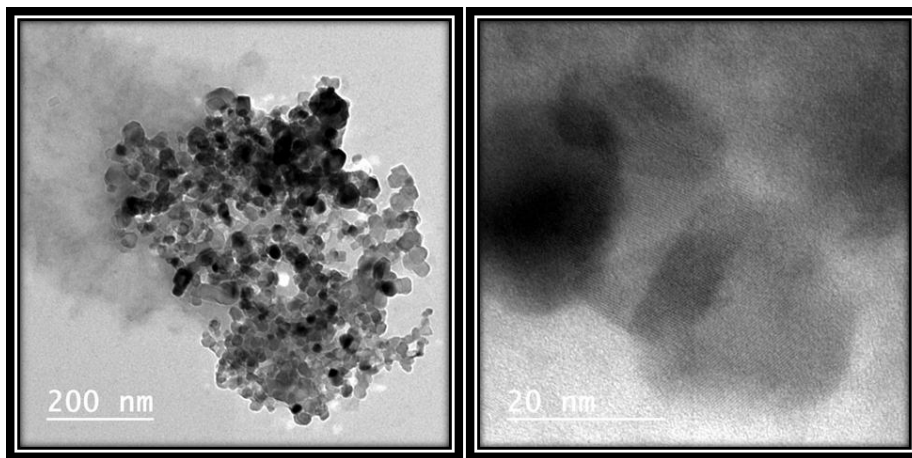


Figure (4): HRTEM images of SPO compound as a powder form with different magnifications

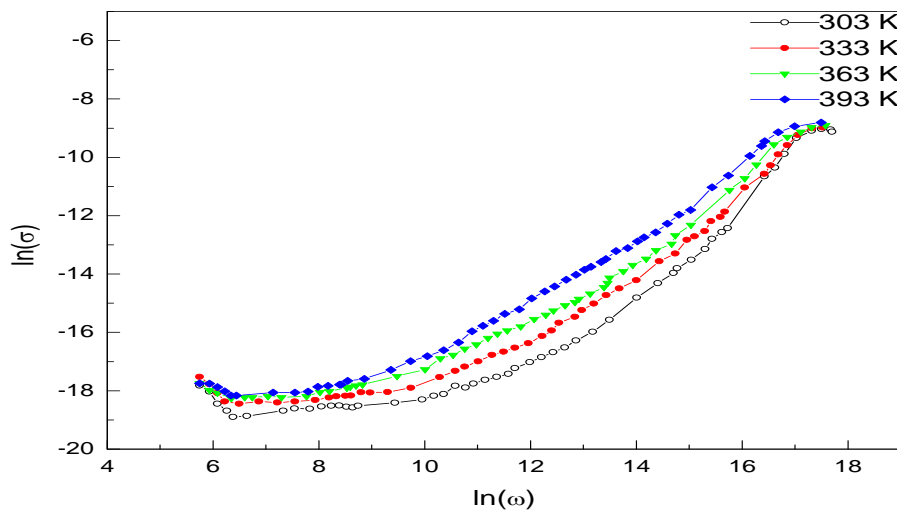


Figure (5): AC conductivity variation versus frequency of SPO at different temperature

It can be seen, for all temperatures, that the AC conductivity can be divided into 3 regions. The low frequency region from 50Hz. to about 1KHz. Intermediate frequency region, from 1KHz. to 1MHz, is recognized as region 2. Region 3 is designated for the high frequency region above 1MHz. up to 5MHz. In region 1, the AC conductivity is frequency independent, whilst it is slightly temperature dependent. For region 2, is called dispersion region, the AC conductivity strongly depends upon the frequency of the applied electric field and tends to increase with increasing the frequency. Finally, in region 3, the high frequency region, the AC conductivity neither frequency nor temperature dependent.

In the low frequency region, the applied field is not enough to initiate the hopping conduction. In accord only, the conduction mechanism is attributed to drift of carriers and no extra carrier were created. In Consequently the conductivity in this range behaves independently of the frequency of the applied field. In region 2 the frequency of the applied field is enough to initiate and starts the hopping conduction.

In region 2, in which the conductivity linearly increases with increasing the frequency of the applied field, the AC conductivity obeys a power law of frequency according to the relation[27]:-

$$\sigma(\omega) = A\omega^s \quad (3)$$

where A , s and ω are constant, a constant called frequency exponent factor has values between $0 < s < 1$ and the angular frequency, respectively. In order to extract the frequency exponent, factor s a plot between $\ln\sigma(\omega)$ and $\ln(\omega)$ is plotted, in the dispersion region, as depicted in Figure (3) for different temperatures. The s parameter can be extracted at a different temperature from the slopes of each temperature. It's clear that, the values of s were found to increase slightly with increasing temperature, as shown in Figure (6). Regarding to the values of S and its variation against temperature and following S. R. Elliot. 1987, the suitable model is the small Polaron (S.P) [28].

The dispersion formula of the AC conductivity can be expressed as[29]: -

$$\sigma(\omega) = \sigma_h + \left[\frac{(\sigma_L - \sigma_h)}{(1 + (\omega\tau)^2)} \right] \quad (4)$$

where σ_L , σ_h and τ are the conductivities at low and high frequency limits and τ is the relaxation time, respectively. Substituting by $\sigma(\omega)$, σ_h , σ_L and ω in equation (4) the relaxation time τ can be calculated. The variation of the relaxation time τ with different temperature of SPO compound is displayed in Figure(7). It can be observed that the relaxation time tends to increase with increasing temperature and the value of τ is in order $\sim 6-18 \times 10^{-8}$ Sec.

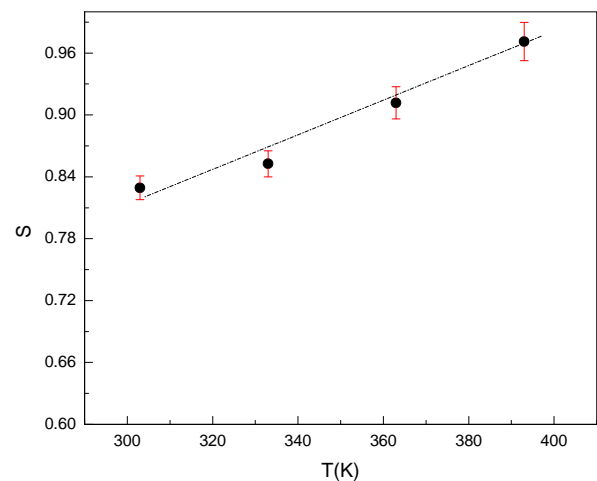
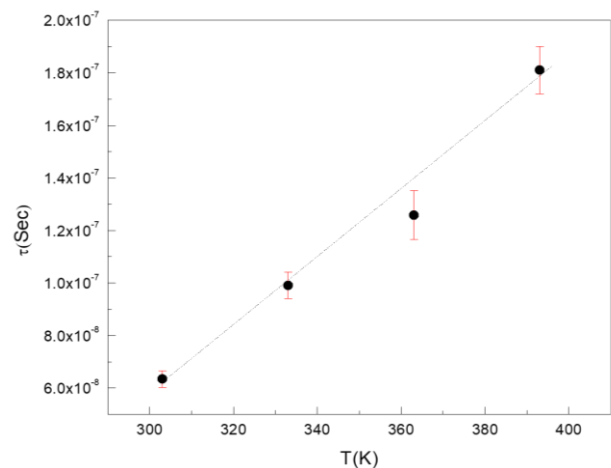


Figure (6): Temperature dependence of the frequency exponent factor of SPO at different temperature



Figure(7): Temperature dependence of the relaxation time, τ , exponent factor of SPO at different temperature

From the temperature dependence of the AC conductivity of SPO as illustrated in Figure (8), the AC activation energy, ΔE , can be calculated according the Arrhenius relation as follows: -

$$\sigma = \sigma_0 e^{-\Delta E/KT} \tag{5}$$

According to the figure (8) with equation (5), the AC activation energy was estimated from the slopes at different frequencies. The activation energy for SPO was found to be in order of 0.2 eV.

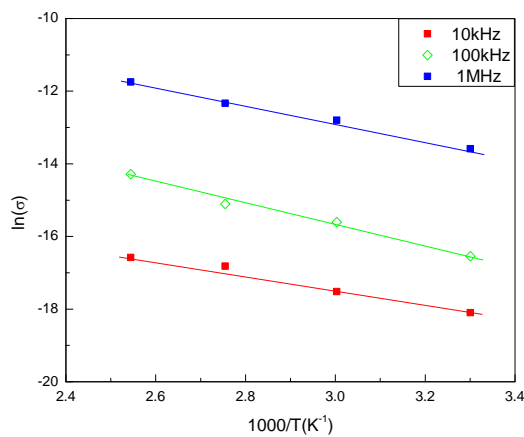
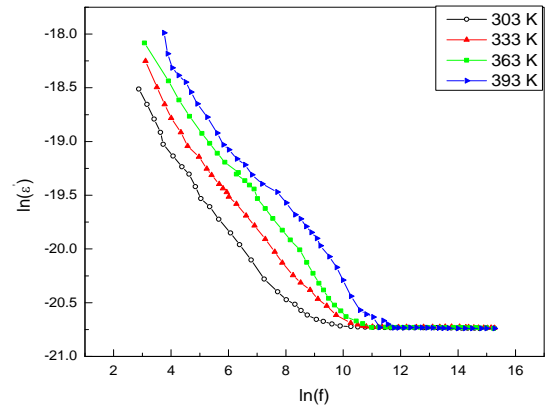


Figure (8): Temperature dependence of the AC conductivity of SPO at different frequencies

The dielectric properties of SPO compound were studied. This investigation concerns the effect of frequency of the applied field and temperature. The dielectric properties include the dielectric constant, ϵ' , the dielectric loss, ϵ'' , and the loss tangent, $\tan \delta$. Such parameters are so important for the industrial applications.

Figure (9) depicts the frequency dependence of the dielectric constant, ϵ' , at different temperatures of SPO pellet. As shown, for all studied temperature over the whole range of frequency, the dielectric constant continuously decreases with increasing the frequency of the applied voltage up to a certain frequency. Above a certain frequency, a saturation part was existed. This behavior may be ascribed to the increase of orientational polarization which might take long time. Also, the dielectric constant ϵ' increases with increasing temperature in the frequency range below ~60 KHz. Whilst, in the low frequency region, above ~100 KHz, the dielectric constant, ϵ' , found to be temperature and frequency independent. Such an increase in

dielectric constant may be described as if the polarization requires less time at higher temperatures. Consequently, the reorientation cannot spontaneously respond to the applied frequency.



Figure(9): Frequency dependence of the dielectric constant at different temperatures for SPO compound

Dielectric loss, ϵ'' , is a measure of the power losses by the sample when an alternating voltage is applied. Figure (10) represents the variation of the dielectric losses of SPO versus frequency of the applied voltage at different temperature. It is obvious that the dielectric loss is frequency dependent, where it decreases with increasing frequency.

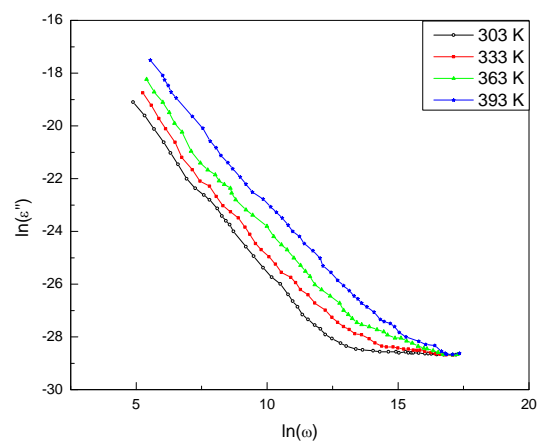


Figure (10): Variation of the dielectric loss of SPO pellet against the applied field frequency at different temperature

In addition, the dielectric loss appears to be dependent on temperature. It can also be seen that the decrease of ϵ'' with frequency may be

represented by the following relations [29], in the frequency range between 100Hz and 60KHz.

$$\varepsilon'' = B\omega^m \quad (6)$$

$$m = -\frac{4k_B T}{W_M} \quad (7)$$

where B, m and W_M are a constant, another frequency applied power factor and the maximum barrier height (the energy required to move the electron from a site to the infinity), respectively. Regarding to the equation (6) and Figure (10), the power, m , can be calculated from the slope of the obtained straight lines part. The values of m should be negative and increase with increasing temperature showing a linear behavior. The calculated values of W_M were found to be decreased from 0.27 to 0.22 eV as the temperature increased from 303 to 393 K, see Table (1).

Table (I): Calculated values of m and W_M for SPO compound at different temperature

T(K)	m	W_M (eV)
303	0.42	0.26971
333	0.43526	0.27542
363	0.54329	0.24053
393	0.6148	0.22012

Loss tangent ($\tan\delta$) is a sample dimension independent dielectric parameter. The value of loss tangent is very important from the applied aspect point of view. Figure (11) shows the frequency dependence of $\tan\delta$ against the frequency of the applied electric field at different temperatures for the investigated SPO pellet. It can be seen, in the low frequency region, the loss tangent decreases sharply with increasing frequency, while it is frequency independent in the high frequency region above 20 KHz. On the other, the loss tangent increases with increasing temperature.

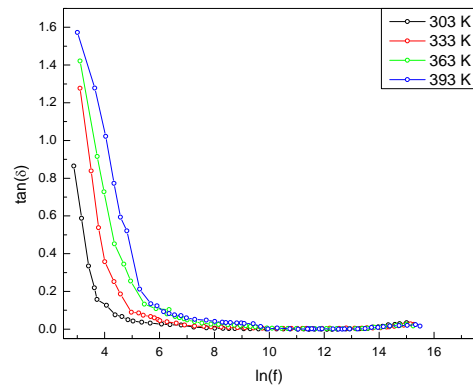


Figure (11): Loss tangent variation against frequency of SPO pellet at different temperatures

Finally, It should be mentioned here that there is a lack of data about the electrical properties of SPO compound specially the AC conductivity and the dielectric properties therefore there was no data to compare with the data reported here.

Conclusion

The XRD, HRTEM, AC conductivity and dielectric properties of SPO pellets have been investigated. XRD suggests that SPO is a monoclinic polycrystalline structure with space group P21 at room temperature. The crystallite size, D , and the strain, ε , were estimated using the Size-strain plot method and the results found to be 34 nm and 67.2×10^{-4} . The high-resolution transmission electron microscope (HRTEM) images confirm the formation of nano-crystalline with diameter range between 30 to 40 nm. In addition, the electrical conductivity and dielectric properties of SPO bulk in the temperature range (303–393 K) and frequency range (50Hz–5 MHz).

AC conductivity suggests that the conduction mechanism of SPO compound is predominantly by small Polaron (S.P) type of conduction. The activation energy and the relaxation time, τ , are found to be around ~ 0.2 eV and $\sim 6-18 \times 10^{-8}$ Sec, respectively. The Values of dielectric constant and dielectric loss of SPO decrease by increasing frequency, at constant temperature, and increase by increasing temperature at constant frequency. Finally, the values of m and W_M were calculated at different temperatures.

References

- 1-Klajn, G.R. Spiropyran-based dynamic materials. *Chem. Soc. Rev.*43(2014) 148.
- 2-Seiler V., Tumanov N., Robeyns K., Wouters J., Champagne B. and Leyssens T., *Crystals* 7 (2017)84.
- 3-El-Nahass M.M. and Desoky W.M., *Applied Physics A* 123 (2017) 517.
- 4-Ye J., Wang L., Wang H., Chen Z., Qiu Y and Xie H., *RSC Adv.* 7 (2017) 642.
- 5- Steven M. P. and Andrew D. T, *Dyes and Pigments*,104 (2014) 123.
- 6-Jianyong Y., Yizhong Y., Xiaohui T., Jinyu S., and Ya G, *J. Phys. Chem. C*, 120 (2016) 14840.
- 7-El-Nahass M.M. and Desoky W.M. *Optik - International Journal for Light and Electron Optics* 171 (2018) 44.
- 8-Yuan Shi Yi, Liang Wu, Jun Gao and Ming Shi J. *OF MACROMOLECULAR SCIENCE, PART A: PURE AND APPLIED CHEMISTRY* 0(2017) 1.
- 9-Kristina Seiler V., Tumanov N., Robeyns K., Wouters J., Champagne B. and Leyssens T., *Crystals*7(2017) 84.
- 10-Levy D., *Mol. Cryst. Liquid Cryst.* 297 (1997) 31.
- 11-Goudjil K. and Sandoval R., *Sens. Rev.* 18 (1998) 176.
- 12- Levy D., de Monte F., Otón J. M., Fiskman G., Matías I., Datta P., and López-Amo M., *J. Sol-Gel Sci. Technol.* 8 (1997) 931.
- 13-Van Gemert B. and Bergoni M. P., *US Patent* 5 066 (1991) 818.
- 14- Knowles D. B., *US Patent* 5 238 (1993) 981.
- 15-Pissadakis S., Anglos D., Klini A. and Konstantaki M., 2011 International Workshop on Bio- photonics, Parma, 8-10 June (2011) 1.
- 16- Huang Y., Liang W., Poon J. K., Xu Y., Lee R. K. and Yariv A., *Applied Physics Letters* 88 (2006) 181102.
- 17-Bonefacino J., Vincent Tse M., Jeff Pun C., Cheng X., Edward W. C., Boersma A., Hwa-Yaw, *Optics and Photonics Journal* 3 (2013) 11.
- 18-Feczkoa T., Kovács M., Voncinad B., *J. of Photochemistry and Photobiology A: Chemistry* 247 (2012) 1.
- 19-J. Harada, Y. Kawazoe and K. Ogawa, *Chem. Commun.*, 46 (2010) 2593.
- 20- Green M. A., Emery K., Hishikawa Y. and W. Warta, *Progr. Photovoltaics* 19 (2011) 84.
- 21-Brabec C. J., Gowrisanker S., Halls J. J. M., Laird D., Jia S. and Williams S.P., *Adv. Mater.* 22 (2010) 3839.
- 22- Krebs F. C., Nielsen T. D., Fyenbo J., Wadstrom M. and Pedersen M. S., *Energy Environ. Sci.* 3 (2010) 512.
- 23-El-Nahass M.M., El-Zaidia E.F., Darwish A.A.A. and Salem G.F. *J. of Electronic Materials*, 46 (2017) 2.
- 24-R. Shirley R., *The CRYSFIRE System for Automatic Powder Indexing: User's Manual*, The Lattice Press, Guildford, Surrey GU2 7NL, England, 2000.
- 25-Laugier J., Bochu B., *LMGP-Suite of Programs for the Interpretation of Xray Experiments*, ENSP/Laboratoire des Matériaux et du Génie Physique, BP 46.38042, Saint Martin d'Herès, France, 2000.
- 26-Khorsand Zak A., Abd. Majid W.H, Abrishami M.E, Yousefi R., *Solid State Sciences* 13 (2011) 251.
- 27-Tomlin S.G, Khawja E. and Thhutupalli G.K., *J. Phys.C: Solid State Phys*, 9 (1976) 4335.
- 28-S. R. Elliott., *Adv. Phys.*, 36 (1987) 135.
- 29-Seyam M.A.M., Bekheet A.E. and Elfalaky A., *Eur. Phy. J. AP*, 16(2001) 99.